SURFACE AND INTERFACE PHONON POLARITONS CHARACTERISTICS IN InAlGaN QUATERNARY ALLOYS

ALJAMEEL, ABDULAZIZ IBRAHEEM A

UNIVERSITI SAINS MALAYSIA
2016

SURFACE AND INTERFACE PHONON POLARITONS CHARACTERISTICS IN InAlGaN QUATERNARY ALLOYS

By

ALJAMEEL, ABDULAZIZ IBRAHEEM A

Thesis submitted in fulfillment of the requirements for the degree of Doctor of Philosophy

MARCH 2016

ACKNOWLEDGMENTS

All glory belongs to Allah the Almighty, the all Knowing and Seeing He alone can guide. I thank Allah subhana wa ta'ala for bestowing his mercy on me, and for guiding me. I could never have accomplished this study without the faith which I have in the Allah Almighty. I send blessings and salutations to His Messenger and his *Ahl*.

I would like to express my sincere appreciation and heartfelt thanks to my main supervisor, Prof. Dr. Haslan Abu Hassan for his creative guidance, intellectual support, stimulating discussions and inspiring words. I am grateful for his excellent hospitality and wonderful attitude. I would also like to acknowledge my co-supervisor, Dr. Ng Sha Shiong for his concern in this work.

Great thanks for Universiti Sains Malaysia for providing me financial support for this research. In addition, I would like to express my gratitude to the School of Physics, Universiti Sains Malaysia. I would also like to acknowledge my own university; Al-Imam Muhammad Ibn Saud Islamic University for their supports.

I would also like to express my appreciation to the staff in the Nano Optoelectronics Research Laboratory for their co-operation, technical assistance and valuable contribution to my work.

Finally, words may not be sufficient to express acknowledgment and my deepest thanks to my parents for their long time support, to my father, who wished to attend with me this great moments (may Allah have mercy on him). I thank my brothers and sisters for their support throughout my study period. Last, and most important, I extend special thanks to my wife and my children for accompanying me during this important time in our lives. I thank them for their support and great patience with me.

TABLE OF CONTENTS

LIST OF TABLES

LIST OF FIGURES

LIST OF SYMBOLS

$\perp$	Direction perpendicular to *c*-axis
$\parallel$	Direction parallel to *c*-axis
A	Hexagonal wurtzite structure
B	Cubic zinc-blende structure
$\gamma_{LO(TO)}$	Longitudinal (Transverse) optical phonon damping constant
γ_p	Plasma damping constant
$\varepsilon_{xx\ (yy)}$	Dielectric tensors perpendicular to *C*-axis
ε_{zz}	Dielectric tensors parallel to *C*-axis
ε_∞	High frequency dielectric constant
ε_0	Vacuum permittivity
ε_{vac}	Dielectric constants of vacuum
$\varepsilon_{\parallel(\perp)}$	Dielectric function parallel (perpendicular) to the *C*-axis
$\varepsilon_{0\parallel(\perp)}$	Dielectric constant static parallel (perpendicular)
$\varepsilon_{\infty\parallel(\perp)}$	High-frequency dielectric constant parallel (perpendicular)
$\varepsilon\ (\mathrm{AC})_{\parallel(\perp)}$	Dielectric constants parallel and perpendicular for AC binary compound
$\varepsilon\ (\mathrm{BC})_{\parallel(\perp))}$	Dielectric constants parallel and perpendicular for BC binary compound
Ω	Angular frequency
θ	Angle of incidence in the medium of incidence
θ_c	Critical angle
Λ	Wave length
ω_{LO}	Longitudinal optical phonon frequency

ω_{TO}	Transverse optical phonon frequency
ω_p	Plasma frequency
a,c	Lattice constants
$A_1(LO_1)$	Phonon mode (longitudinal-optical)
$A_1(LO_2)$	Phonon mode (longitudinal-optical)
E_g	Energy band gap
$E_{x(y,z)}$	Electric field components along the *x-(y-,z-)* direction
$E_1(LO)$	Phonon mode (longitudinal-optical)
$E_1(TO)$	Phonon mode (transverse-optical)
$E_2(L)$	Phonon mode (low)
$E_2(H)$	Phonon mode (high)
$k_{\|\|}$	In-plane wavevector component of evanescent wave generated by ATR crystal
k_{vac}	Wavevector of the vacuum light line
k_x	Wavevector of SP along the *x*- direction
l	Specifice layer in amultilayer system
m	Interface between layer l and layer l+1
N	Refractive index
n_p	Refractive index of the ATR crystal
N	Total number of layers
$\boldsymbol{Q}$	wave-vector
H_y	Magnetic field
$r_{s,p}$	S- and P-polarized IR reflection coefficient
R	Reflectivity
X	In composition

Y	Al composition

LIST OF MAJOR ABBREVIATIONS

AlN	Aluminum nitride
AlInN	Aluminum indium nitride
AlGaN	Aluminum gallium nitride
ATR	Attenuated total reflection
a.u.	Arbitrary unit
BPP	Bulk phonon polariton
BZ	Brillouin zone
C_{6v}^4	Space group
CL	Cathodoluminescence
e-beam	Electron beam
EM	Electromagnetic
eV	Electron volt
EW	Evanescent wave
FTIR	Fourier Transform Infrared
InN	Indium nitride
InGaN	Indium gallium nitride
InAlGaN	Indium aluminum gallium nitride
IRE	Internal reflecting element or (IR Ellipsometry)
IPP	Interface phonon polariton
GaAs	Gallium arsenide
GaN	Gallium nitride
Ge	Germanium
KBr	Potassium bromide
KOH	Potassium hydroxide

LED	Light Emitting Diode
LD	Laser Diode
LO	Longitudinal optical
LST	Lyddan-Sachs-Teller
MBE	Molecular beam epitaxial
MgO	Magnesium Oxide
MM	Mixed mode behaviour
OM	One-mode behaviour
PA-MBE	Plasma assisted molecules beam epitaxy
PBN	Pyrolytic boron nitride
PL	Photoluminscence
QW	Quantum well
RF	Radio frequency
RHEED	Reflection high energy electron diffraction gun
Si	Silicon
SiC	Silicon carbide
SiO_2	Silicon dioxide
SP	Surface polariton
SPP	Surface phonon polariton
TD	Threading dislocation
TE	Transverse electric
TEM	Transmission electron microscopy
TGS	Triglycine sulfate
TM	Two-mode behaviour or Transverse magnetic
TO	Transverse optical

UHV	Ultra high vacuum
UV	Ultra Violet
VIS	Visible
ZB	Zinc blend structure
ZnSe	Zinc selenide

CIRI-CIRI POLARITON FONON PERMUKAAN DAN ANTARAMUKA DI DALAM ALOI KUATERNARI InAlGaN

ABSTRAK

Dalam projek ini sifat-sifat optik dua set filem nitrida kuaternari telah dikaji secara eksperimen dan teori. Set pertama ialah nitrida kuaternari $In_xAl_yGa_{1-x-y}N$ dengan aluminum (Al) malar, y=0.06 dan pecahan mol indium (In) yang berubah dalam julat $0 \leq x \leq 0.10$, sementara set kedua dengan In malar, x=0.10, dan komposisi Al yang berubah dalam julat $0 \leq y \leq 0.20$. Dalam kajian ini pelbagai peralatan pencirian tak sentuhan dan tak memusnahkan telah digunakan. Ini merangkumi spektroskopi pantulan inframerah (IR) terkutub dan pantulan penuh dilemahkan IR terkutub (ATR) bagi pencirian optik. Dalam kategori pertama projek ini, ciri spektra pantulan inframerah (IR) terkutub dan ciri optik $In_xAl_yGa_{1-x-y}N$ telah dikaji. Berasaskan model fungsi dielektrik anisotropik, spektra pantulan IR eksperimen telah dipadankan secara berangka oleh spektra pantulan IR teori. Persetujuan yang baik telah diperolehi antara spektra yang diukur dengan spektra yang dikira. Daripada padanan lengkung-lengkung eksperimen, parameter-parameter reststrahlen di pusat zon Brillouin dapat ditentukan. Dalam kategori kedua, sifat-sifat polariton fonon permukaan (SPP) dan kesan komposisi aloi, x, dan y ke atas SPP aloi ternari dan quaternari telah dikaji. Skop kajian merangkumi kedua-dua pendekatan teori dan kajian eksperimen supaya dapat menyumbang kepada pemahaman sifat-sifat asas bahan. Hubungan sebaran polariton permukaan (SP) dikaji secara teori berasaskan satu model anisotropi. Keputusan menunjukkan bahawa mod SPP $Al_xGa_{1-x}N$, $In_xGa_{1-x}N$ dan $Al_xIn_{1-x}N$ bersandar kuat kepada komposisi Al dan In, x, dan kelakuan mod SPP $Al_xGa_{1-x}N$ dan $In_xGa_{1-x}N$ dapat diklasifikasikan sebagai kelakuan

satu-mod (OM), sementara mod SPP bagi $Al_xIn_{1-x}N$ dapat diklasifikasikan sebagai kelakuan campuran-mod (MM). Kelakuan mod SPP di dalam aloi kuarternari $In_xAl_{0.06}Ga_{1-x-0.06}N$ dapat diklasifikasikan sebagai kelakuan dua-mod dan wujud dalam dua cabang, A dan B. Dapat dilihat dengan jelas bahawa frekuensi mod polariton fonon antaramuka (IPP) secara beransur-ansur berkurangan apabila *x* meningkat bagi semua cabang. Data juga menunjukkan kebersandaran mod SPP kepada komposisi Al bagi aloi kuaternari $In_{0.10}Al_yGa_{1-0.10-y}N$ dalam dua cabang (bagi *y=0.05* sahaja), iaitu cabang A dan B. Dapat dilihat dengan jelas bahawa frekuensi mod SPP dalam cabang A secara beransur-ansur berkurangan apabila *y* meningkat dan mod SPP tersebut mempamerkan kelakuan MM. Juga dapat dilihat secara jelas bahawa frekuensi mod IPP secara beransur-ansur berkurangan apabila *y* meningkat sehingga ke y=0.10 dan kemudian mod IPP secara beransur-ansur meningkat apabila *y* terus meningkat. Namun begitu, sifat-sifat bahan bagi bahan aloi yang terbentuk adalah bersandar kepada komposisi aloi dan secara biasanya dapat diwakili oleh satu interpolasi linear atau tak linear di antara juzuk-juzuknya.

SURFACE AND INTERFACE PHONON POLARITONS CHARACTERISTICS IN InAlGaN QUATERNARY ALLOYS

ABSTRACT

In this project the optical properties of two sets of quaternary nitride films have been investigated experimentally and theoretically. The first set is the quaternary nitride $In_xAl_yGa_{1-x-y}N$ with constant aluminum (Al), y=0.06 and varied indium (In) mole fraction ranging from $0 \leq x \leq 0.10$, while the second set is with constant In, $x = 0.10$, and variable Al composition ranging from $0 \leq y \leq 0.20$. In this study various non-contact and non-destructive characterization tools were used. These include polarized infrared (IR) reflectance and polarized IR attenuated total reflection (ATR) spectroscopy for optical characterization. In the first category of this work the features of the polarized IR reflectance spectra and the optical characteristics of $In_xAl_yGa_{1-x-y}N$ were investigated. Based on the anisotropic dielectric function model, the experimental IR reflectance spectra were numerically fitted by the theoretical IR reflectance spectra. Good agreement between the measured and calculated spectra has been obtained. From the fit of the experimental curves, the reststrahlen parameters at the center of Brillouin zone were determined. In the second category, the surface phonon polariton (SPP) properties and the effect of the alloys composition, x, and y on the SPP for ternary and quaternary alloys were investigated. The scope of study covers both theoretical approach and experimental works in order to contribute to the understanding of the fundamental properties of the materials. The surface polariton (SP) dispersion relations were studied theoretically based on an anisotropy model. These results indicate that the SPP modes of $Al_xGa_{1-x}N$, $In_xGa_{1-x}N$ and $Al_xIn_{1-x}N$ are strongly dependent on the Al and In compositions, x,

and the behaviour of the SPP modes of $Al_xGa_{1-x}N$ and $In_xGa_{1-x}N$ can be classified as one-mode (OM) behaviour, while for the $Al_xIn_{1-x}N$ the SPP mode can be classified as mixed-modes (MM) behaviour. The behaviour of the SPP mode in the $In_xAl_{0.06}Ga_{1-x-0.06}N$ quaternary alloys can be classified as two-mode behaviour and existed in two branches, A and B. It is clearly seen that the frequency of the interface phonon polariton (IPP) mode gradually decreases as the *x* increases for all branches (SPP and IPP). The data also shows the Al composition dependence of the SPP modes for the $In_{0.10}Al_yGa_{1-0.10-y}N$ quaternary alloys in two branches (at y=0.05 only), branch A and B. It is clearly seen that the frequency of the SPP mode in branch A gradually decreases as the *y* increases and the SPP mode exhibits MM behaviour. Also it is clearly seen that the frequency of the IPP mode gradually decreases as *y* increases up to y=0.10 and then the IPP mode gradually increases as the *y* further increases. However, the material properties of the alloy materials formed are dependent on the alloy composition and typically can be represented by a linear or non-linear interpolation between its constituents.

CHAPTER 1

INTRODUCTION

1.1 Introduction for III-nitrides and InAlGaN

InN, GaN, and AlN, as well as their ternary and quaternary compounds such as AlGaN and InAlGaN, are referred to as group III-nitride semiconductors. Their crystals form wurtzite, zincblende, and rocksalt structures. Almost all device applications are based on wurtzite crystals, which is the most thermodynamically stable form of these semiconductors. Recently and due to their applications in electronics and optoelectronics in the blue and ultraviolet (UV) regions of the light spectrum such as UV sensors, the wide-band gap semiconductors based on binary group III-nitrides, such as AlN, GaN, InN, and their alloys have attracted huge attention. The III-nitrides have attracted interest because of the lack of semiconductors that satisfy the commercial needs for light emitting diode (LED) devices and green, blue, and UV lasers. The continuous alloy systems formed by III-nitrides with direct band gaps extends from 0.7 eV (for InN) to 3.4 eV (for GaN) and to 6.2 eV (for AlN), which cover the technologically important UV and visible spectral ranges [1–5].

However, the performance of nitride laser diodes (LDs) will be reduced by large lattice mismatches relative to GaN (e.g., from 2.4% tensile for AlN and 11% compressive for InN). The strain in ternary nitride alloys is due to the lattice mismatching with the substrates. The corresponding piezoelectric and spontaneous polarization, produces a total polarization field in the range of megavolt per centimeter [6,7] which reduces the radiative recombination rates and optical gain coefficients in the active layers. To enhance the properties of these devices a zero

total field at every interface must be found. Under this condition, the nitride Laser Diodes (LDs) will improved their properties such as; reducing the threshold currents, increasing output powers, and prolonged lifetimes.

The III-nitride ternary alloys, particularly AlGaN, are potential candidate materials in semiconductor light emitting devices, solar-blind UV detector, and sensor devices, particularly for applications under harsh environment conditions. These alloys can also cover the spectrum from the visible to deep-UV spectral range. These characteristics are strongly driven by their physical properties such as excellent chemical, mechanical, and thermal stability and unique optical properties, such as direct and tunable band gap energy (3.4 eV to 6.2 eV) [8–13].

The III-nitride quaternary InAlGaN alloys have been proved to be good compounds to cover many gaps of other binary and ternary nitride alloys because the lattice parameters and the energy band gap are under controlled in the quaternary alloys. For instance, by changing the (In) and (Al) contents (*x* and *y*, respectively) in the quaternary $In_xAl_yGa_{1-x-y}N$ alloys, the band gap energy can be changed and GaN-based lattice matched structures can be reached. Furthermore, $In_xAl_yGa_{1-x-y}N$ can also thermally match with GaN, and this enhances the growth condition because it provides greater flexibility in the devices. For device application, the InAlGaN can produce improved lattice matching to the cladding layer which enhance UV emission efficiency. The increasing in the emission efficiency in InAlGaN quaternary alloys is nearly thrice as compared to the AlGaN ternary alloys.

Ternary $In_xGa_{1-x}N$, $Al_xIn_{1-x}N$ or $Al_xGa_{1-x}N$ and quaternary $In_xAl_yGa_{1-x-y}N$ compounds can also cover band gaps corresponding to light emission from IR to the whole visible range, even to certain UV range. Thus, these alloys are good candidates for lighting and data storage applications.

The applicability of III-nitrides can be extended with the growth of $In_xAl_yGa_{1-x-y}N$ alloys. $In_xAl_yGa_{1-x-y}N$ alloys have been investigated as LDs in the UV region [14], light-emitting diodes (LEDs) [15], and QWs based on that alloy, which show high luminescence intensity.

1.2 Introduction for surface phonon polariton

The surface phonon polariton (SPP) properties have recently gained considerable attention as a specific field of research. Surface phonon polariton (SPP) is an elementary excitation resulting from the coupling of an infrared (IR) photon (with transverse magnetic mode) with a transverse-optic (TO) phonon in polar crystals.

New applications based on the unique characteristics of SPPs have emerged. For example, Balin *et al*. (2009) [16] demonstrated a reflection-type sensor in the mid-infrared (IR) region based on resonant excitation of SPPs.

In addition, SPP is applied for some photonic devices [16–19] and near-field microscopy [20, 21]. The production of SPP mode is coming from the coupling between photon and phonon, especially between a transverse magnetic (TM) mode of IR photon and a phonon with a transverse optic (TO) mode in polar crystals. SPP is a surface mode because it propagates along the interface between two different media. This propagation will be parallel to the surface of the crystal with amplitude exponentially attenuated from the surface to the bulk. Another unique characteristic of the SPP is that it can found in the forbidden band of the bulk phonon polariton (BPP) modes. This forbidden band found between the transverse optic (TO) and longitudinal optic (LO) phonon frequencies. The SPP enhance the surface IR absorption.

Recently, the SPP mode properties of III-nitride binary and ternary alloys have much investigated [22–33], but the optical properties such as the phonon mode behavior have a few experimental report. In addition, quaternary nitrides are very complex alloys and cannot be described by the same properties of wurtzites. Nitrides are currently grown heteroepitaxially because bulk InAlGaN and other III-nitride semiconductors are still not available. The SPP characteristics in a InAlGaN heterostructure system have not been explored.

Understanding the surface and interface phenomena is very important in fabrication of multi-junction semiconductors device. In a semiconductor multilayer system, the properties of the surface and interfaces tend to dominate over the bulk properties of each layer. The interfaces in semiconductor heterostructure yield dramatic changes in many fundamental properties, such as the electron transport and optical phonon properties [34–37].

1.3 Objectives of this research

The principal goal of this work is to study the behavior of the SPP in wurtzite $In_xAl_yGa_{1-x-y}N$ quaternary alloys. The effects of the variation of alloy composition (i.e., x and y) on the SPP and IPP are investigated. The scope of study covers the theoretical approach and experiments to determine the fundamental properties of this material. The initial efforts mainly focused on theoretical investigation, which includes simulation of the SP dispersion curves by using an anisotropy model and identification of the origin of each SP branch.

Recent studies have verified the theoretical results with relevant experimental data. These studies include the determination of the optical parameters by polarized IR reflectance measurement; verification of observed features in the *p*-polarized IR

attenuated total reflection (ATR) experiments by comparing experimental data with theoretical simulations; and extraction of information about the SPP mode from the ATR spectra with the aid of the SP dispersion curves. In addition, the specific objectives in this project include:

1. Studying the behavior of the SPP in wurtzite $In_xAl_yGa_{1-x-y}N$ quaternary alloys using theoretical and experiments approaches.

2. Studying the effects of the increase in In mole fraction with constant Al (y=0.06) on the optical properties [optical phonon, SPP, and interface phonon polariton (IPP) modes] of quaternary $In_xAl_yGa_{1-x-y}N$ nitride semiconductor samples.

3. Studying the effects of the increase in Al mole fraction with constant In (x=0.10) on the optical properties (optical phonon, SPP, and IPP modes) of quaternary $In_xAl_yGa_{1-x-y}N$ nitride semiconductors.

4. Comparing the theoretical and experimental optical properties between these two groups of samples.

1.4 Originality of the research works

The main originality in this study is in the experimental and theoretical investigations of the influences of the alloy compositions on the SPP and IPP modes of two sets of $In_xAl_yGa_{1-x-y}N$ thin films. The first set has constant Al (y=0.06) and In in the range of $0 \leq x \leq 0.10$, whereas the second set has constant In (x=0.10) and variable Al composition ranging from $0 \leq y \leq 0.20$. The composition dependence and the behavior of the SPP and IPP modes of $In_xAl_yGa_{1-x-y}N$ thin films are reported for the first time.

Moreover, some new findings, mainly the composition dependence equation for the optical phonon modes, have been derived. In addition, the results of this

research have also provided new explanations for the origin of the optical phonon modes that can be obtained by oblique incident polarized IR measurements on the wurtzite nitrides. In polarized IR spectroscopy, the behavior of the electromagnetic field at the sample surface is enhanced.

1.5 Outline of the thesis

The content of this dissertation is organized as follows. Chapter 2 introduces an overview of the wurtzite III-nitrides, which include binary (GaN, AlN, and InN), ternary ($Al_xGa_{1-x}N$, $In_xGa_{1-x}N$, and $Al_xIn_{1-x}N$), and quaternary ($In_xAl_yGa_{1-x-y}N$) materials. However, the behavior of the BZ optical phonon modes and the SPP mode are the focal points. In addition, an overview of the assignment of the IR optical phonon modes will be presented.

Chapter 3 reports the basic principles of the ternary and quaternary materials systems. Special attention is given to the characteristics of the crystalline structure, BZ optical phonon modes, and SPP mode of these alloys. Moreover, theoretical models are used to fit/generate the polarized IR reflectance and the ATR spectra. The simulations of the SP dispersion curves of the $In_xAl_yGa_{1-x-y}N$ semiconductors are also included in this chapter.

In Chapter 4, the basic principles of the characterization tools, process equipments, and materials are discussed. These data include the experimental details for each instrumental setup, operating conditions and resolution, and the sample details. The polarized IR reflectance of wurtzite $In_xAl_yGa_{1-x-y}N$ thin films are investigated experimentally and theoretically in Chapter 5.

Chapter 6 discusses the results of the theoretical studies on the composition dependence of the SPP mode on wurtzite structure characteristics for AlGaN, InGaN,

and AlInN ternary alloys over the whole composition range. Moreover, the SPP and IPP characteristics of wurtzite ($In_xAl_yGa_{1-x-y}N$) thin films are investigated experimentally by *p*-polarized IR ATR spectroscopy. The theoretical SP dispersion curve and the theoretical *p*-polarized IR ATR spectra are simulated using the standard matrix formulation; the film and substrate anisotropy are considered.

In Chapter 7, the conclusions of the research are presented. Several recommendations for future studies are also included.

CHAPTER 2

LITERATURE REVIEW

2.1 Introduction

In this chapter, an overview of the III-nitride binary, ternary, and quaternary alloys, as well as the polarized IR active optical phonon modes of wurtzite InAlGaN thin films, is presented. The SPP mode of the III-nitrides semiconductor will also be reviewed.

2.2 Overview of the binary III-nitrides

Information technology nowadays is built on semiconductors compounds and their electronics. For a few years ago, computers and networks have facilitated the revolution in telecommunication, transportation, and the like. The fast development in semiconductors could meet the urgent demands of this electronic technology.

For several years silicon-based devices have been further developed and to date have represented the core of the entire semiconductor industry. However, the recent developments have reached the theoretical limit of silicon, such as temperature (150 °C) and breakdown voltage (300V) limits, thus leading to the need of using other semiconductors with properties that cannot be reached by using silicon.

The III-nitrides, specifically GaN, AlN, InN, and their compounds, have been extensively studied due to their important applications in semiconductor devices, electronics, and optoelectronics that operate in the blue and UV regions of the light spectrum. The focus on the III–V nitrides is due to the lack of semiconductor

compounds that can meet commercial demands for blue, green, and UV lasers and light-emitting devices. The direct energy band gap range of these continuous alloy systems extends from 0.7eV (for InN), 3.39 eV (for GaN), to 6.2 eV (for AlN), thereby covering the technologically important UV and visible spectral ranges [1].

The first binary alloy to be discussed is GaN, which is a direct and wide-band gap semiconductor. This alloy is a suitable semiconductor material for devices in high-temperature, caustic environment, and space applications because of its superior radiation hardness and chemical stability, as well as its large band gap. GaN is also effective as a protective coating because of its radiation hardness [1]. Its wide band gap caused its operation temperature to be naturally much higher than other materials such as Ge, Si, and GaAs. Given that the intrinsic carrier concentration at any given temperature decreases exponentially with the band gap, GaN is an attractive material for high-temperature applications.

Moreover, GaN exhibits higher sheet charge densities, higher mobilities, enhanced charge confinement, and higher breakdown voltages compared with other semiconductors. Thus, GaN is suitable for application in electronic devices for high-temperature, high-power, and high-frequency transistors [38–40].

The transparency of high-quality GaN at wavelengths longer than the band gap makes the alloy an ideal material for fabricating photodetectors that can reject near-IR and visible regions of the solar spectrum and simultaneously retain near unity quantum efficiency in the UV. Moreover, in optoelectronics, GaN is basically important for its potential as a blue and UV light emitter [1].

The semiconductor compound crystal structure is determined by the main properties of the compound. The GaN and other III-nitrides compounds commonly display a wurtzite crystal structure. Although the other structure rock-salt or

zincblende structure is also depending on the growth experimental conditions and the on the substrates, the most thermodynamically stable is the wurtzite structure. While at high external pressure the wurtzite is transformed to zincblende structure in some cases. Thus, the zincblende structure is metastable, while if it epitaxial growth on Si, GaAs, MgO, and 3H SiC it may be stabilized. However, the majority of studies have high a tension on the hexagonal wurtzite crystal phase because the growth of the wurtzite structure is easier and has low cost than that of the cubic structures. In fact, the hexagonal structure is stable and can be grown on different type of substrates, such as Al_2O_3, SiC, and Si [41,42].

Figure 2.1 illustrates the hexagonal wurtzite structure; the edge length of its base is *a*=3.189 Å and its lattice heights is c=5.185 Å [43].

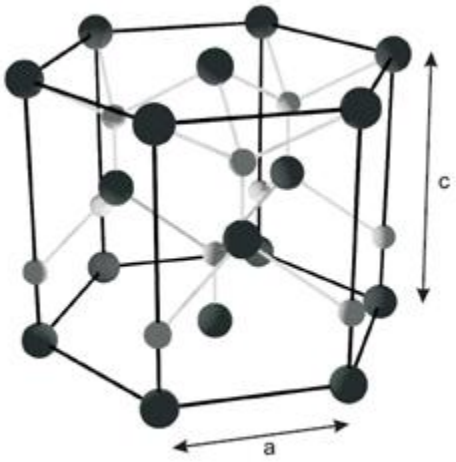

Figure 2.1: Wurtzite crystal structure of GaN [43].

Table 2.1 summarizes most of the properties of wurtzite and zincblende GaN, which are important for electronic devices. These properties include the wide band gap and high critical electric field. GaN is very stable structurally and chemically because the

Ga and N atoms have strong ionic bonds to build the GaN compound, this bond energy is about 8.92 eV/atom.

Table 2.1: Comparison between the properties of GaN, Si and AlN [40, 44]

Parameters	**Si (Diamond)**	**AIN (Wurtzite)**	**GaN**	
			Wurtzite	**Zinc Blende**
Lattice Constant (Å)	a = 5.43	a = 3.112 c = 4.982	a = 3.189 c = 5.185	a = 4.50
Energy gap (Ev)	1.12	6.2	3.39	3.2
Density (g / cm^3)	2.33	3.23	6.15	
Number of atoms (cm^{-3})	5.0×10^{22}	9.59×10^{22}	8.9×10^{22}	
Static Dielectric Const.	11.9	8.5	8.9	9.7
Optical Phonon Energy (meV)	63	99.2	91.2	87.3
Breakdown field (Vcm^{-1})	$\sim 3 \times 10^5$	$1.2 \sim 1.8 \times 10^6$	$\sim 5 \times 10^6$	
Electron Mobility (cm^2 / Vs)	1500	300	~1000	
Hole Mobility (cm^2 / Vs)	450	14	~200	~350
Refractive Index	3.42	$n_\infty = 2.15$	$n_\infty = 2.3$ (2.3~2.45 over visible range)	$n_\infty = 2.3$
Melting Point (°C)	1415	3000	~2500	
Thermal Conductivity (W / CM °C)	1.5	2.85	1.3	
Thermal Expansion Linear ($°C^{-1}$)	$\alpha = 2.6 \times 10^{-6}$	$\alpha_\alpha = 2.6 \times 10^{-6}$ $\alpha_\beta = 2.6 \times 10^{-6}$	$\alpha_\alpha = 2.6 \times 10^{-6}$ $\alpha_\beta = 2.6 \times 10^{-6}$	

The second binary alloy is the hexagonal AlN, which has an ultra-wide direct band gap (*Eg*=6.2 eV) among the III-nitride compounds. AlN has melting point about (3000 °C), thermal conductivity near (2.85 W/cm·°C), high thermal stability, large dielectric constant, high hardness, and excellent electrical insulating property [45,46]. Furthermore, the most widely accepted lattice constants of the crystal structure of wurtzite AlN are *a*=3.112 Å and *c*=4.982 Å [47].

AlN has the potential applications for microelectronic and optical devices. This alloy is necessary for high-power applications because of its high thermal conductivity. In addition, AlN is used as a buffer layer in the growth of multiple QW structures and in a highly efficient superlattice cladding layer [48,49]. To date, the third binary InN and its alloys have become very important basically because of the recent breakthrough in InN epitaxial technology and it has a narrow direct band gap of 0.7 eV–1.0 eV [50–53]. Accordingly, InN can be possibly replaced Si in Si-based devices.

2.3 Overview of the ternary III-nitrides

By changing the Al concentration in the $Al_xGa_{1-x}N$ ternary alloys ($0 \leq x \leq 1$), the direct energy band changes from 3.4 eV (360 nm in GaN) to 6.2 eV (200 nm in AlN). Consequently, new applications have emerged for AlGaN-based devices, such as in optoelectronic devices, UV photodetectors, and sensors, particularly under harsh environmental conditions [54].

The ternary semiconductor $In_xGa_{1-x}N$ is a suitable candidate because of the active layer in the violet-, blue-, and green-based LEDs and LDs. Its band gap covers these spectral regions depending on the In mole fraction used. The miscibility gap between InN and GaN leads to the formation of In-rich nanoclusters in the InGaN

QWs. Thus, the In-rich nanoclusters will appear as potential minima for the electrons in the conduction band and holes in the valence band. If these potential minima are deep enough, then the electrons and holes will be trapped inside, resulting in confined transitions. These transitions have been proposed to have caused many of the anomalous luminescence properties of InGaN. If the carriers are localized in these potential minima, then they are protected from the non-radiative recombination centers (such as dislocations). This characteristic would help explain the efficient luminescence observed in these devices in very high densities (~1010 cm^{-3}) of threading dislocations (TDs) [55,56]. These TDs act as non-radiative centers in the GaN layer [57].

The properties and growth of ternary AlInN compound are being intensively examined, primarily for electronic applications, given their band gap changing from energy gap of AlN at 6.2 eV to InN at 0.7 eV. Ternary AlInN alloys have much attention for application as an active layer in LEDs and LDs operating from UV to IR spectrum. Moreover, $Al_{0.83}In_{0.17}N$ can be used as a cladding buffer layer with no strain on a GaN-based LD structure. This characteristic leads to a reduction in the defects because it is lattice constant has the same as in GaN [58,59].

2.4 Overview of the quaternary III-nitrides

New materials known as quaternary nitrides are created by connecting InN with GaN and AlN. The band gap of the resulting alloys can be increased from 0.7 eV for InN to 6.2 eV for AlN, which is critical for fabricating high-efficiency light sources and optoelectronic devices as shown in figure 2.2. Only limited information has been published concerning the InAlGaN quaternary system.

Nowadays quaternary III-nitrides compound have much attention as active layers in visible and UV LEDs and LDs. In particular, the use of quaternary InAlGaN offers the advantage of independently selecting the lattice parameter and the band gap energy of the film.

InAlGaN compound is particularly important because it has a strong spontaneous UV emission intensity caused by an enhanced radiative recombination of localized excitons/carriers, as previously clarified for InGaN-based emitters. These results were confirmed by transmission electron microscopy (TEM) and cathodoluminescence (CL) [60]. The existence of In-rich nanoclusters at room temperature is to enhance the optical properties of InAlGaN layers, and also responsible for the confinement of the electron-hole pairs created by the promotion of valence electrons into the conduction band [61].

Hence, the emission efficiency of the quaternary alloy is approximately thrice as high as that of the AlGaN ternary alloys as comparable Al composition [62]. Therefore, an effect similar to that obtained in InGaN QWs is expected for InAlGaN quaternary alloys [63].

Hirayama et al. [64] found that the addition of 3%–5% In to AlGaN alloys can increase the PL emission by three orders of magnitude relative to that of the AlGaN layer without In. This increase is attributed to the In segregation into quantum dots. The emission resulting from the InAlGaN is almost as strong as the best quality InGaN.

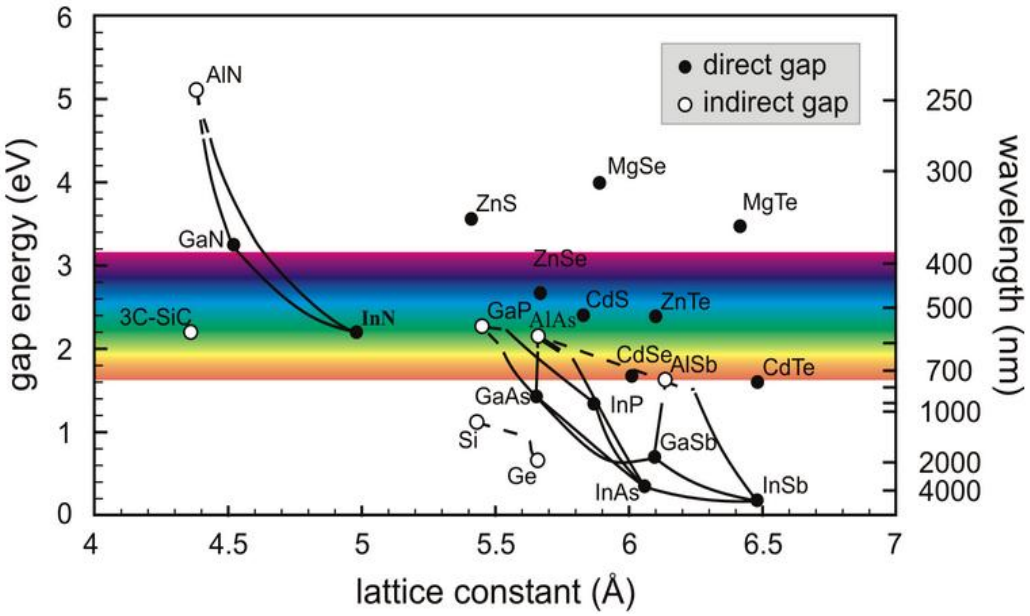

Figure 2.2: Band gaps of the most important elemental and binary cubic semiconductors versus their lattice constant at 300 °K. The right-hand scale gives the light wavelength λ, corresponding to the band gap energy [1].

2.5 Overview on polarized IR active optical phonon modes of wurtzite GaN-based ternary and quaternary thin films

Since wurtzite structure GaN is a uniaxial crystal, two sets of phonon parameters are required to describe the dielectric function (ε), namely, one set to model $\varepsilon_{\perp}$ and another set to model $\varepsilon_{\parallel}$ [65]. According to Dumelow et al. [66], the materials parameters can be determined more accurately if the reflectance measurements are performed by means of the oblique incidence polarized light. In the phonons propagation there are two phonon modes, the first is the TO phonon mode which is perpendicular to the crystal axis (c) $\varepsilon_{\perp}$, while the second mode is the LO which is parallel to c-axis $\varepsilon_{\parallel}$.

Detailed investigations of the polarized IR reflectance on GaN were reported by Barker and Ilegems (1973) [67], Manchon et al. (1970) [68], Sobotta et al. (1992) [69], Hao et al. (1999) [70], Wetzel et al. (1996) [71], Mirjalili et al. (1996, 1998) [72,73], and Yu et al. (2004) [74]. In addition, numerous polarized IR

ellipsometry (IRE) measurements on GaN thin films have been reported. However, the interpretation of the spectra and the ways to extract the lattice vibrational parameters are different from the typical polarized IR reflectance analysis. Thus, it will not be discussed here.

The optical parameters with large uncertainty have been determined in the early investigation of the GaN thin films (most probably of poor quality) by Barker and Ilegems (1973) and Manchon et al. (1970) [67,68]. Sobotta et al. (1992) [69] measured GaN samples with crystallographic *c*-axis along the plane of the layers. They determined the exact optical parameters from the reflectivity spectra for the polarizations perpendicular ($\boldsymbol{E} \perp c$) and parallel ($\boldsymbol{E} \parallel c$) to the *c*-axis. Hao et al. (1999) [70] studied the polarized transmission and reflection measurements of bulk GaN, but their analyses were mainly on the determinations of absorption coefficient and refractive index. Wetzel et al. (1996) [71] studied the polarized IR reflection of heterostructures of GaN and AlGaN thin films with AlN buffer layers. However, their studies mainly focused on the LO phonon modes of GaN and AlN. Mirjalili et al. (1996, 1998) [72,73] reported the polarized IR measurements of GaN films with various structures that are deposited on various substrates. However, as commented by Hao et al. (1999) [70], the simulated spectra do not exactly fit the experiment well enough. Yu et al. (2004) [74] studied the polarized IR reflection of GaN epilayer grown on sapphire substrate at three different angles of incidence (18°, 45° and 75°). Their studies focused on the fitting of the numerical first differential reflectance using a factorized model of dielectric constant, and more attention was given to the sapphire. For GaN thin films on sapphire, they were unable to observe and fix the A_1 (TO) phonon mode, and an A_1 (TO) mode with a large uncertainty was obtained.

In addition, a set of TO ($\perp$ and ||) and LO ($\perp$ and ||) phonon modes for both $\boldsymbol{E} \perp c$ and $\boldsymbol{E} \parallel c$ has been determined. Principally, the $TO_{\perp}$ and $LO_{\parallel}$ are first obtained from the best fits of the theoretical model to the experimental curve, and then Lyddane–Sachs–Teller (LST) relation [75] is applied to calculate the corresponding $LO_{\perp}$ and $TO_{\parallel}$. To date, good agreement has been obtained between the reported results, which are deemed to be accurate. However, the fundamental principle of the IR phonon coupling is apparently not considered. In typical IR measurements, the wave-vector ($\boldsymbol{q}$) of the radiation may be taken as zero ($\boldsymbol{q}$=0). This characteristic is often referred to as the "long-wavelength limit" or "zone-center" approximation [76,77]. Consequently, the optical phonon modes that can be detected are those coming from the BZ center only, namely, the $TO_{\perp}$ and the $LO_{\parallel}$, whereas the BZ edge modes of $LO_{\perp}$ and $TO_{\parallel}$ are forbidden. Notably, the condition also holds for Raman scattering [77]. As a result, the interpretation of the polarized IR reflectance spectra and the use of the LST equation should be explored for determination of the $LO_{\perp}$ and the $TO_{\parallel}$ phonon modes. Studies on the origin of the $TO_{\parallel}$ phonon mode in the *p*-polarized spectrum thus far is insufficient. According to the Balkanski IR theory for thin films [78], Fresnel formulae for the oblique incidence polarized IR reflectivity, and vector analysis of the polarized IR incident beam, this mode actually has the same origin as the TO mode in the *s*-polarized spectrum and can be attributed to the $TO_{\perp}$ optical phonon mode.

In general, most of the studies are performed by using Raman methods. This is because Raman spectroscopy is a direct technique for the observation of optical phonons as compared to the IR and IRE spectroscopy. Unlike the Raman approaches, a fitting procedure is normally needed to extract the phonon frequencies from the IR

and IRE spectra. The work of extraction may become complicated if the reststrahlen band (IR absorption band) of the concerning layer is superimposed with that from the underlying layer. Nevertheless, in some aspect, the IR or IRE spectroscopy is preferred than the Raman scattering. For instance, they are more sensitive to the IR-active lattice vibration modes as compared to Raman scattering measurement.

2.6 Overview of SPP mode

The general principles of the excitation of surface waves by Attenuated Total Reflection (ATR) spectroscopy were proposed and described by Otto (1968) [79]. Since then, their properties in GaAs film, GaP thin slabs, and in different systems (mostly for the alkali halides such as CdF_2, CaF_2, NaF, LiF, and MgF_2) have been extensively investigated. Detailed accounts are discussed in a number of books and review articles [80–83].

In the past few decades, studies on SPP have been conducted via the ATR on CdTe epilayers on GaAs substrate [84], GaAs/AlAs superlattice [85], and GaAs/$Al_xGa_{1-x}As$ multiple QW structures [86].

Recently, the optical properties in GaN-based ternary and quarterly mixed crystals have been widely investigated. The fundamental surface properties (SPP mode) have not received sufficient attention and are still relatively unexplored. Studies on the SPP of AlN are still rare, because most studies are devoted to GaN.

2.6.1 Overview of SPP mode of the binary III-nitrides

For wurtzite GaN, the pioneer work was carried out by Torii et al. (2000) [87] by means of experimental and theoretical studies. For *s*-polarized beam, no evidence of the appearance of the SPP mode has been found. For the *p*-polarized beam,

however, an absorption peak attributed to the SPP mode of the GaN was clearly observed at 699 cm^{-1}, which is in good agreement with the theoretical results. For cubic GaN, Davydov et al. (1997) [88] reported on the surface and IPP of cubic GaN which grown on (001) GaAs substrates using Raman scattering. A small peak due to cubic GaN of the SPP mode was detected at 709 cm^{-1}, this peak is matching with the theoretical prediction.

The SPP mode of AlN is rarely reported. Ng et al. (2007) [35] conducted theoretical and experimental studies on the SPP mode of the wurtzite AlN thin films for the first time. In the experimental measurements the *p*-polarized IR ATR measurements were performed. A strong absorption dip corresponding due to the SPP mode of AlN was noted at 839.0 cm^{-1}. In other hand the SP dispersion curve of the AlN thin film was simulated theoretically. The difference in SPP values between the theoretical and experimental measurements was less than 2%. More details can be found in Ng et al. (2007) [35]. The SPP on the vacuum–AlN interface was reported and discussed [89-91]. This interface exists in almost the same band as sapphire SPP, and the TO frequencies of AlN [92,93] appear in the dispersion region of sapphire SP. Thus, the resonance of sapphire substrate SP with TO phonon of AlN film can be detected.

Ng et al. (2010) [94] studied the SPP and IPP of InN thin films which grown on Si(111) substrate, a buffer layer of AlN was also grown epitaxaly using MBE. SPP and IPP modes of InN/AlN/Si sample were detected by the *p*-polarized IR ATR techniques. Two peaks were noted at 609 and 877 cm^{-1} which are due to SPP and IPP of InN respectively. The origins of the observed peaks were verified by theoretical simulations based on the anisotropic model. In general, a good agreement

between the experimental and theoretical results was obtained for *p*-polarized infrared attenuated total reflection study of InN thin films.

Regardless of the extensive studies on the growth and measurements of the electrical and optical properties of InN, only a little simulation and experimental studies on its SPP characteristics have been reported [95–97]. One of these studies offered by Ng et al. (2008, 2009), they studied theoretically of the SPP mode of wurtzite (α) InN and $In_xGa_{1-x}N$ ($0 \leq x \leq 1$) [95,96], whereas Bao and Liang (2006) reported on the SPP characteristics of cubic (β) structure $In_xGa_{1-x}N$ ($0 \leq x \leq 1$) [97].

2.6.2 Overview of SPP mode of the ternary III-nitrides

Recently, the SPP modes of III-nitride ternary alloys and their mixed crystals have been studied [98-100]. Bao and Liang reported a theoretical simulation studies on the SPP mode of InGaN ternary alloys [101], they found that the SPP mode in InGaN ternary alloys exhibits a one-mode behavior. For wurtzite α-$In_xGa_{1-x}N$ ternary compounds over all composition, Ng et al. (2008) [95] reported a theoretical study on the SPP mode and their dependence on the composition. These SPP modes were obtained using theoretical simulations by applying an anisotropy model. Their results revealed that the SPP mode found in a one-mode behavior. Thus, the SPP mode dependent on the composition of α-$In_xGa_{1-x}N$ semiconductors with bowing parameter of $-28.9\ cm^{-1}$ is theoretically obtained.

Moreover, Ng et al. [96] investigated the SPP characteristics of AlGaN thin film systems by experiments and found an obvious absorption dip of SPPs in *p*-polarized IR ATR measurements. To the best of the researcher's knowledge, a small number of publications have reported on the study of SPP mode of the $Al_xGa_{1-x}N$ thin films as well as the influences of the alloy composition on the SPP mode of these alloys. For

other ternary alloys, such as $Al_xGa_{1-x}As$, $In_xGa_{1-x}N$, and $Zn_xCd_{1-x}S$, only the theoretical results are reported [101,102].

In the case of the $In_xGa_{1-x}N$ ternary alloys, the theoretical study is based on a cubic lattice (NaCl structure) model. Bao and Liang (2006) [101] discussed that to get more accurate results they must used an anisotropy model $In_xGa_{1-x}N$ (as well as the other III-nitride systems) that has a wurtzite structure in nature. However, the fundamental SPP characteristics of ternary AlInN alloys remain unclear.

2.6.3 Overview of SPP mode of the quaternary III-nitrides

The quaternary InAlGaN alloys are promising materials that offer several advantages over GaN, InGaN, and AlGaN alloys [103]. This is because it allows the independent control of lattice constant and energy band gap. For example, by varying indium (In) and aluminum (Al) compositions *x* and *y* in $In_xAl_yGa_{1-x-y}N$, one can change the energy band gap while GaN-based lattice matched structures can be obtained [104]. In addition, it also has the potential to provide a better thermal match to GaN, which could be an important advantage in epitaxial growth and hence, giving much greater flexibility in the design of devices. In terms of devices applications, the InAlGaN can produce improved lattice matching to the cladding layer and better ultra-violet emission efficiency [105]. The above characteristics are also true for ternary and binary nitrides, however the emission efficiency of the quaternary alloys is about three times higher than the AlGaN ternary alloys with a comparable Al composition [103]. Besides that it offer a similar emission effect to that obtained in InGaN quantum wells (QWs) [106,107].

In general, the phonon mode behavior of the quaternary nitrides has not been widely studied experimentally. In addition, quaternary nitrides are very complicated

and cannot be explained by the same method of wurtzite structure. To help understand the fundamental properties of this material, Ng et al. (2010) [108] investigated experimentally and theoretically the SPP in $In_{0.04}Al_{0.06}Ga_{0.90}N/AlN/Al_2O_3$ quaternary semiconductors. However, the experimental results of the phonons mode of quaternary samples are still incomplete. Moreover, no consensus exists as to whether the InAlGaN with a one-, two-, or mix-mode behavior should be considered.

The SPP mode of the III-nitride quaternary semiconductors is rarely reported Hence, thorough studies on the surface properties of this quaternary alloy system are urgently need.

2.7 Summary

In this chapter, wurtzite binary (GaN, AlN, and InN), ternary (AlGaN, InGaN, and AlInN), and quaternary nitrides (InAlGaN) are reviewed briefly. The reviews focused on the energy band gap and related bowing parameter and the behavior of the BZ optical phonon modes, followed by brief explanations on the polarized IR active optical phonon modes and the SPP modes.

CHAPTER 3

FUNDAMENTAL PROPERTIES AND THEORETICAL MODELS

3.1 Introduction

In this chapter, the basic principles of ternary and quaternary materials systems are presented. Special attention is given to the characteristics of the crystalline structure, the Brillouin zone (BZ) optical phonon modes, and the SPP modes of these alloys. In addition, theoretical models used to fit the polarized IR reflectance as well as the *p*- polarized ATR and SP dispersion curve of the $In_xAl_yGa_{1-x-y}N$ semiconductors are also included. Simulations of the SP dispersion curves are introduced. The simulations are achieved by initially determining the dielectric tensor components of the studied material. Therefore, a description of the dielectric function model used in this study is given first. Finally, a summary of this chapter is presented.

3.2 Fundamental properties of the ternary $Al_xGa_{1-x}N$, $In_xGa_{1-x}N$ and $Al_xIn_{1-x}N$

In general, the III-V binary compounds deal with only a limited range of materials properties, for instance, lattice parameters and band gap energy. For many technological applications, material properties that are intermediate between those offered by the individual III–V binary compounds are desirable. Conventionally, such desirable effects can be achieved through alloying, that is, amalgamation of two or more binary compounds. The material properties of the alloy materials formed depend basically on the alloy composition and are obtained typically based on interpolation. Studies on the physical properties of the AlGaN ,InGaN and AlInN

alloys are useful not only fundamentally, but also for a better understanding of their structure and optical properties.

3.2.1 BZ optical phonon modes of $Al_xGa_{1-x}N$

The distribution of the atoms in the ideal case of the ternary nitrides $Al_xGa_{1-x}N$ alloy is as follows: N atoms occupy the anion sites, whereas Al and Ga atoms share the cation sites with a probability ratio *x: (1-x)*. Given that the optical phonon for Raman and FTIR spectra are generally highly sensitive to disorder in atomic arrangements [109]. In general, optical phonon characteristics in such ternary semiconductor $AB_{1-x}C_x$ can be classified into three classes, according to the behavior of their zone-center optical phonons: one-mode, two-mode, and mixed mode (MM) [110]. One-mode behavior appears as one set of LO and TO phonons where the frequencies are linearly proportional with compositional x. By contrast, in the two-mode behavior the phonon modes split into two sets of phonons LO and also two for TO phonon. Each set is referring to one component as a lighter and a heavier component of the two binary semiconductors, i.e., AC and BC, which represent the compositional extremes of the ternary system. The mixed mode behavior has a mixture of the one-mode and two-mode behavior.

3.2.2 BZ optical phonon modes of $In_xGa_{1-x}N$

Both hexagonal GaN and $In_xGa_{1-x}N$ have the wurtzite structure with two formula units per primitive unit cell. As described in Chapter 2, the III-nitrides have a wurtzite or zincblende structure. For example, the primitive cell of hexagonal structure consists of two pairs of atoms like Ga–N atom in the hexagonal GaN, but in the cubic structure there is only one atom pair. The length of a unit-cell in the cubic structure along the axis [111] is determined only by the width of one unit bilayer, but